Biogeosciences, 10, 3679–3689, 2013
www.biogeosciences.net/10/3679/2013/
doi:10.5194/bg-10-3679-2013

Biogeosciences Open Access

Response of bacterioplankton community structure to an artificial gradient of pCO_2 in the Arctic Ocean

R. Zhang[1,2,*], X. Xia[1,2,*], S. C. K. Lau[3], C. Motegi[4], M. G. Weinbauer[4], and N. Jiao[1,2]

[1]State Key Laboratory of Marine Environmental Science, Xiamen University, Xiamen 361005, China
[2]Institute of Marine Microbes and Ecospheres, Xiamen University, Xiamen, 361005, China
[3]Division of Life Science and Division of Environment, The Hong Kong University of Science and Technology, Clear Water Bay, Kowloon, Hong Kong SAR, China
[4]Microbial Ecology and Biogeochemistry Group, Université Pierre et Marie Curie-Paris 6, Laboratoire d'Océanographie de Villefranche, 06230 Villefranche-sur-Mer, France; CNRS, Laboratoire d'Océanographie de Villefranche, 06230 Villefranche-sur-Mer, France
[*]These authors contributed equally to this work.

Correspondence to: R. Zhang (ruizhang@xmu.edu.cn) and N. Jiao (jiao@xmu.edu.cn)

Received: 28 July 2012 – Published in Biogeosciences Discuss.: 9 August 2012
Revised: 16 April 2013 – Accepted: 29 April 2013 – Published: 4 June 2013

Abstract. In order to test the influences of ocean acidification on the ocean pelagic ecosystem, so far the largest CO_2 manipulation mesocosm study (European Project on Ocean Acidification, EPOCA) was performed in Kings Bay (Kongsfjorden), Spitsbergen. During a 30 day incubation, bacterial diversity was investigated using DNA fingerprinting and clone library analysis of bacterioplankton samples. Terminal restriction fragment length polymorphism (T-RFLP) analysis of the PCR amplicons of the 16S rRNA genes revealed that general bacterial diversity, taxonomic richness and community structure were influenced by the variation of productivity during the time of incubation, but not the degree of ocean acidification. A BIOENV analysis suggested a complex control of bacterial community structure by various biological and chemical environmental parameters. The maximum apparent diversity of bacterioplankton (i.e., the number of T-RFs) in high and low pCO_2 treatments differed significantly. A negative relationship between the relative abundance of *Bacteroidetes* and pCO_2 levels was observed for samples at the end of the experiment by the combination of T-RFLP and clone library analysis. Our study suggests that ocean acidification affects the development of bacterial assemblages and potentially impacts the ecological function of the bacterioplankton in the marine ecosystem.

1 Introduction

Microorganisms are a key component in marine planktonic food webs (Azam et al., 1983). Eukaryotic phytoplankton and cyanobacteria contribute significantly to photosynthesis and primary production in the ocean. Heterotrophic bacteria and archaea process approximate half of the primary production and recycle organic and inorganic nutrients. These microbial functions are crucial components in several major concepts of marine food web structure and organic matter cycling, e.g., the microbial loop and microbial carbon pump (Azam et al., 1983; Jiao et al., 2010).

Generally, microbial diversity and community structure are controlled by abiotic and biotic factors. For example, bacterial communities are affected by the spatial and temporal dynamics of environmental parameters. Nutrient availability and water characteristics (e.g., temperature, salinity and pH) contribute to microbial biogeography in the ocean (Martiny et al., 2006). Considering the changing oceanic conditions induced by anthropogenic impacts (including climate change), it is necessary to investigate whether and how the microbial communities would respond to the emerging changes, and to evaluate the possible ecological consequences of the microbial responses. Such hitherto unknown information is crucial to our understanding and predictions of the possible effects of global climate changes to the biosphere (IPCC, 2007).

A consequence of increasing CO_2 in the atmosphere is a decrease of pH in the water (ocean acidification), which has been confirmed by long-term field observation and is related to anthropogenic CO_2 emission (Dore et al., 2009). It is estimated that the pH of global surface seawater will decrease by 0.2 to 0.4 units by the end of this century based on the general emissions scenarios and circulation models (Caldeira and Wickett, 2003). This predicted rate of ocean acidification is greater than those which have occurred over the past 300 million years (Hönisch et al., 2012). Such changes would fundamentally alter ocean chemistry from the surface water to the deep sea. Our understanding of the biological and ecological effects of changing seawater carbonate chemistry is still in its infancy. While it is well recognised that ocean acidification will have serious negative impacts for most marine calcifiers, the increasing pCO_2 effects on non-calcifiers are not clear. For example, positive effects of elevated pCO_2 concentrations were observed for marine autotrophs in the phytoplankton (Riebesell, 2004), suggesting a "CO_2 fertilisation" phenomenon (Hutchins et al., 2009). While similar fertilisation effects occurred for the cyanobacteria *Synechococcus*, the other major cyanobacteria *Prochlorococcus* showed no response to pCO_2 increase (Fu et al., 2007). It appears that autotrophic nitrogen fixers and anaerobic denitrifiers directly or indirectly benefit from ocean acidification (Hutchins et al., 2007, 2009). However, the abundance and/or activity of nitrifiers might be repressed, since nitrification rates declined with rising pCO_2 level in the ocean (Beman et al., 2011).

Thus far, most of our knowledge of ocean acidification on microbes is derived from laboratory experiments with a small number of cultured microbial taxa (Liu et al., 2010), and the knowledge about the response of natural heterotrophic bacterioplankton communities to ocean acidification is scarce (Weinbauer et al., 2011). A general observation was that ocean acidification had no significant influence on bacterial abundance, but affected various activity parameters like bacterial production, extracellular enzyme activities, etc. (Allgaier et al., 2008; Arnosti et al., 2011; Grossart et al., 2006; Newbold et al., 2012). However, the responses of bacterial community composition (BCC) to pCO_2 levels are complex. Newbold and coworkers did not observe a clear change of bacterial community composition under elevated pCO_2 (Newbold et al., 2012), while data from two mesocosms of the PeECE II experiment showed different BCC in low and high pCO_2 treatments (Arnosti et al., 2011). In addition, there is evidence that community structure of free-living bacteria, but not particle-attached ones, changed with the pCO_2 level (Allgaier et al., 2008). Therefore, in the Svalbard 2010 mesocosm experiment of the European Project on Ocean Acidification (EPOCA) (Gattuso and Hansson, 2009), the largest ocean acidification experiment performed so far, BCC was investigated for a better understanding of bacterioplankton response to different pCO_2 treatments.

In the present study, we used terminal restriction fragment length polymorphism (T-RFLP) analysis and clone library analysis to investigate the dynamics of bacterial diversity and community structure during the 30 day mesocosm experiment in Arctic waters. The automatic capillary running, rapid data production and high reproducibility of T-RFLP analysis allowed analysing and comparing large amount of samples (e.g., 159 samples of 19 sampling points from 9 mesocosms in our study). Two companion publications (Roy et al., 2013; Sperling et al., 2013) present the size fraction (particle-attached and free-living) bacterial community dynamics in same mesocosm experiment by using automated ribosomal intergenic spacer analysis (ARISA) and 454-based 16S rRNA amplicon sequencing. These three papers provide the most detailed and systematic description of bacterial community changes in an artificial pCO_2 gradient in marine ecosystem so far.

2 Materials and methods

2.1 Experimental set up and sampling

As a part of EPOCA, the ocean acidification mesocosm experiment was performed in King's Bay (Kongsfjorden), Spitsbergen (78°56.2′ N, 11°53.6′ E). Detailed information of the experimental setup is provided elsewhere (Riebesell et al., 2012). Briefly, nine KOSMOSs (Kiel Off-Shore Mesocosms for Future Ocean Simulations) were deployed on 31 May, 2010 (experimental date: t-7) and closed on experimental date t-5. Each mesocosm was equipped with a 17 m long polyurethane bag (2 m above sea level and 15 m below), containing about 45 m^3 of seawater. CO_2-saturated seawater was added stepwise during t-1 to t-4 and nine pCO_2 concentrations were used in the mesocosms: low pCO_2 levels including 175 (M3), 180 (M7) and 250 (M2) µatm; intermediate pCO_2 levels including 340 (M4), 425 (M8) and 600 (M1) µatm; high pCO_2 levels including 675 (M6), 860 (M5) and 1085 (M9) µatm. The setup of a gradient of pCO_2 levels allows the use of regression statistics and the detection of possible threshold levels for CO_2 sensitive processes. The control (with ambient pCO_2 level) was duplicated (M3 and M7) to reduce the risk of losing the control for the experiment (Riebesell et al., 2012). Nutrients (5 µmol L^{-1} Nitrate, 0.3 µmol L^{-1} phosphate and 2.5 µmol L^{-1} silicate) were added into all mesocosms prior to the sampling on t13 in order to induce the development of a phytoplankton bloom (Schulz et al., 2013).

Environmental parameters (temperature, conductivity, pH, oxygen, fluorescence, turbidity and light intensity) in the mesocosms were measured daily with a CTD60M (Sun and Sea Technologies). Depth-integrated seawater samples (5 L; from surface to 12 m depth) were collected from the mesocosms using HYDRO-BIOS water samplers (Kiel, Germany). The measurements of chemical and biological core parameters are described in Schulz et al. (2013). Microbial cells in freshly collected seawater samples (2 L each) for

bacterial community structure analysis were harvested using membrane filtration (0.22 µm-pore-size Isopore membrane, Millipore). In the present study, sampling was performed on nineteen days during the experiment, with a relatively dense sampling in first half of 30 day period, followed by regular sampling every other day.

2.2 DNA extraction and PCR amplification of bacterial 16S rRNA genes

DNA was extracted following the previously published protocol (Zhang et al., 2007) with some modifications. The filter membranes were deep frozen and thawed three times in liquid N_2 and at 65 °C, respectively. 8 µL of proteinase K (10 mg mL^{-1} in TE buffer) was then added, followed by incubation for 30 min at 37 °C. After that, 80 µL of 20 % SDS was added, followed by incubation for 2 h at 65 °C. After vortexing, an equal volume of phenol-chloroform-isoamylalcohol (25 : 24 : 1 by volume) was added and centrifuged at 10 000 g for 5 min. The upper aqueous layer was transferred into a fresh tube and treated with an equal volume of chloroform-isoamylalcohol (24 : 1 by volume). The mixture was centrifuged at 10 000 g for 10 min, and the upper aqueous phase was transferred into a new tube. Subsequently, 0.6 times volume of isopropanol was added to the aqueous solution and the mixture was incubated at −20 °C for 20 min, and then centrifuged at 12 000 g for 15 min. The DNA was washed with 70 % ethanol and dissolved in 100 µL of sterilized ultrapure water (produced by the Milli-Q academic A10 system). The quality and quantity of the environmental genomic DNA were evaluated by NanoDrop (Thermo Scientific).

The amplification of bacterial 16S rRNA genes for DNA fingerprinting analysis was performed with universal primers 27F (5′-AGA GTT TGA TCC TGG CTC AG-3′), fluorescently labelled with 6-carboxyfluorescein phosphoramidite (Fam), and 907R (5′-CCG TCA ATT CMT TTG AGT TT-3′) (Amann et al., 1995). Each PCR mixture (50 µL) contained 5 µL PCR buffer, 200µM of each deoxynucleoside triphosphate, 0.1 µM of each primer, 1 µL template DNA (about 10 ng µL^{-1}), and 0.5 U of Ex-Taq DNA polymerase (TAKARA, Dalian, China). The thermal cycles were 95 °C for 3 min; 30 cycles of 95 °C for 1 min, 55 °C for 1 min, 72°C for 1 min; and 72 °C for 10 min. PCR products were purified using the QIAquick PCR Purification Kit (Qiagen Inc., Valencia, CA) according to the manufacturer's protocol.

2.3 Terminal restriction fragment length polymorphism (T-RFLP) analysis

Purified PCR products were double-digested with restriction enzymes Msp I and Rsa I (New England Biolabs, Ispswich, MA, USA) according to the manufacturer's protocol. Selected samples were digested only with Rsa I so as to verify that the T-RFLP patterns obtained were the result of double digestion. Aliquots of digested PCR products were mixed with 0.125 µL of the internal size standard (Bioventures MapMarker 1000, Cambio, Cambridge, UK) and analysed using the MegaBACE platform (Amersham). All T-RF analyses were performed using the Genetic Profiler in the MegaBACE software package (Amersham) as described previously (Lau et al., 2005). T-RFs < 50 bp and > 900 bp were excluded from the analysis to avoid detection of primers and uncertainties of size determination, respectively. To normalise the variation of the amount of DNA loaded on the capillary, the percentages of each T-RF peak area compared to the total peak area of each sample were calculated and T-RFs with a peak area less than 1 % of the total peak area were removed for statistical analysis. An improved binning strategy was applied for the remaining T-RFs data matrix following the protocol described previously (Hewson and Fuhrman, 2006).

2.4 Clone library construction and phylogenetic analysis

The bacterial 16S rRNA genes in the $t30$ samples were PCR amplified using the primer set 27F and 1492R (5′-GGC TAC CTT GCC ACG ACT TC-3′) with the same PCR programme as described above (Lane, 1991). The PCR amplicons ($\sim$1500 bp in size) were cloned into the vector with a TOPO TA Cloning Kit (Invitrogen, Carlsbad, California, USA) according to the manufacturer's instructions. The 16S rRNA genes were sequenced from both ends using the primers M13F (5′-GTTGTAAAACGACGGCCAGTG-3′) and M13R (5′-CACACAGGAAACAGCTATG-3′) on an ABI DNA autosequencer. Phylogenetic affiliations of the sequences were determined using the BLASTN programme on the NCBI (http://www.ncbi.nlm.nih.gov) and RDP (http://rdp.cme.msu.edu/) website. The 16S rRNA gene sequences were clustered as operational taxonomic units (OTUs) at an overlap identity cut-off of 97 % sequence similarity. Pairwise comparisons of each clone library were performed using LIBSHUFF (version 0.96; http://www.mothur.org). The DNA sequences obtained in this study are available from GenBank under the accession numbers JN975970-JN976712.

The possible phylogenetic assignment of T-RFs from T-RFLP analysis of environmental samples was performed with in silico digestion of the DNA sequence of clone library. A variation of 1–3 bp, depending on the size of the T-RF, was applied for the comparison between T-RF positions of community-based and sequence-based in silico analysis (Fabrega et al., 2011).

2.5 Statistic analysis

The resultant T-RFLP data matrix (percentage of peak area) were analysed using PRIMER 5 software (Clarke and Gorley, 2001). The similarity between T-RF patterns was calculated using the two-way crossed analysis

of similarities (ANOSIM). The differences were considered significant when $P < 0.05$. The dynamics of bacterial communities were displayed by MDS (multidimensional scaling) analyses, which were based on Log $(x+1)$ transformation of T-RF data and Euclidean distance. The bacterial taxonomic richness was defined as the number of peaks of T-RFLP analysis. The Shannon-Weaver index (H) was calculated as:

$$H = -\sum (P_i \bullet \log P_i) \quad (1)$$

where $P_i = n_i N^{-1}$, n_i is the area of a peak and N is the sum of all peak areas in each sample. The relationship between the measured environmental parameters and the bacterial community structure as revealed by T-RFLP was assessed by the BIOENV analysis provided in PRIMER 5 software. The BIOENV analysis selects the environmental parameters that may best explain the community pattern (presence/absence and area of T-RFs) by maximising the correlation between their respective similarity matrices with the application of a weighted Spearman's correlation coefficient. Due to the different frequencies for sampling for specific parameters and the analysis of T-RFLPs, we could not include all T-RFLP and environmental parameters in BIOENV analysis. Therefore, the following environmental parameters were used for BIOENV analysis: Salinity, temperature, density anomaly, pH, DO (dissolved oxygen), Chl a measured by CTD and fluorometer, A_T (total alkalinity), C_T, pH_CO2SYS, pCO_2_CO2SYS, HCO_3_CO2SYS, CO_3_CO2SYS, Omega Ca_CO2SYS, Omega Ar_CO2SYS, total bacterial abundance, high DNA bacterial abundance, low DNA bacterial abundance, total and four different DNA viral abundance, VBR (viruses-bacteria ratio), POC (particulate organic carbon), PON (particulate organic nitrogen), POP (particulate organic phosphate), nutrient concentration (NH_4^+, NO_3^-, NO_2^-, PO_4^{3-}, and biogenic Si), DMS (dimethylsulfide) and TEP (transparent exopolymer particles). These factors were analysed individually and in combination (Table 1). The potentially collinear factors were excluded in BIOENV analysis with combined factors to avoid possible confounding effects (Zuur et al., 2010).

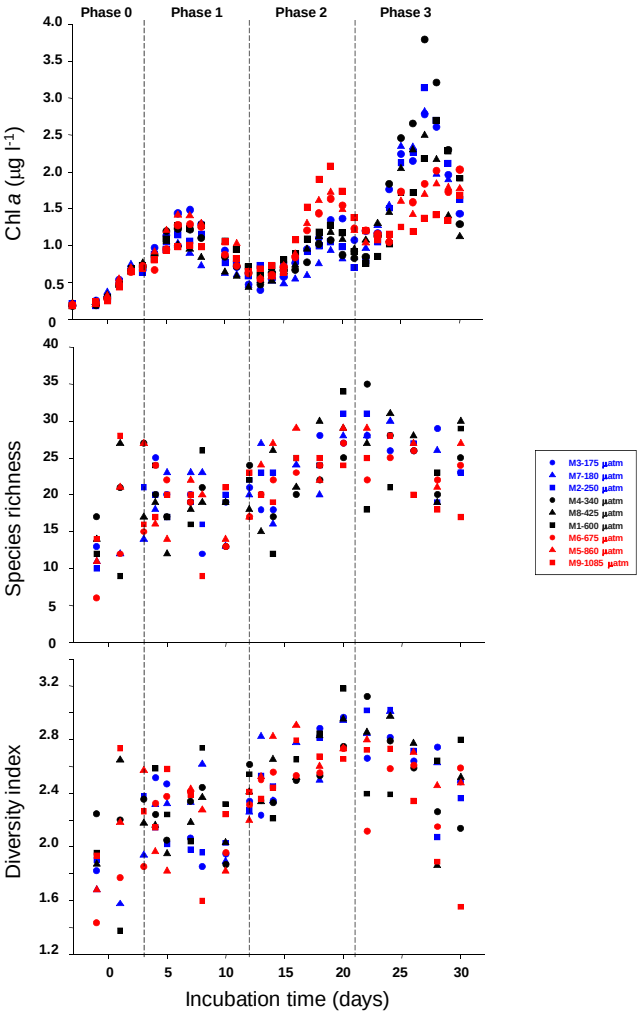

Fig. 1. Time development of Chl a and bacterial diversity during the 30 day mesocosm experiment. Chl a pattern was adapted from Schulz et al. (2013). Bacterial species richness and diversity index were calculated by T-RFLP fingerprinting of bacterial community based on PCR amplified 16S rRNA gene. Four phases based on experimental setup and Chl a concentrations are shown for reference. The low, intermediate and high pCO_2 treatments are displayed with blue, dark and red symbols, respectively.

3 Results

3.1 Bacterial community dynamics revealed using T-RFLP analysis

Four phases were defined based on the experimental setup and the temporal dynamics of Chl a concentration during the 30 day mesocosm experiment (Fig. 1): Phase 0 (CO_2 manipulation period, t-5 to t3), Phase 1 (the first bloom period, t4 to t12), Phase 2 (the second bloom period, t13 to t21) and Phase 3 (the third bloom period, t22 to t30). A detailed description of the development of Chl a is presented in Schulz et al. (2013). Bacterial abundance showed a distinct temporal development with an abruptly drop before t7 followed by gradual increase until the end of experiment (Brussaard et al., 2013).

Apparent taxonomic richness (number of T-RFLPs in each sample) and Shannon-Weaver diversity index calculated using the T-RFLP matrix showed three major phases (Fig. 1). The development of Chl a showed also three phases, however, they occurred on slightly different time scales. Firstly, the apparent bacterial taxonomic richness and the diversity index increased rapidly during the pCO_2 manipulation procedure, peaked at around t3–t5 and then decreased until t10. The first peak and trough of apparent bacterial diversity were ahead of those observed in terms of the Chl a

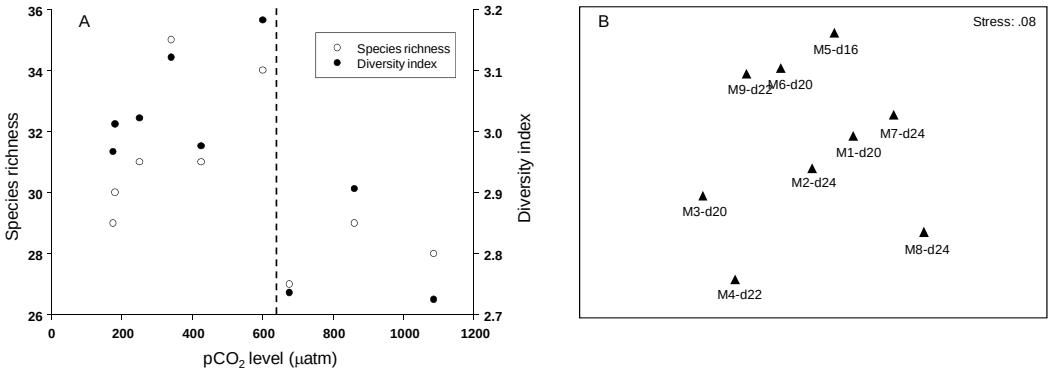

Fig. 2. Effects of pCO_2 levels on the development of the bacterial community structure during the 30 day mesocosm experiment. **(A)** Maximum bacterial taxonomic richness (S_{max}) and diversity index (H_{max}) as revealed by T-RFLP analysis (see materials and methods for the definition of taxonomic richness and diversity index). The possible biological threshold of ocean acidification effects is indicated by a dashed line. **(B)** MDS plotting of bacterial community structures of samples with S_{max}. Similar pattern was observed for samples with H_{max}.

Table 1. BIOENV analysis of similarity matrices of bacterial community structure based on T-RFLP analysis and environmental factors. BIOENV analysis was performed for combined environmental factors to obtain the five highest ranked correlations between similarity matrices of community fingerprints and environmental data. The five individual environmental parameters with highest correlation coefficient values were also shown. DO: dissolved oxygen; BA: bacterial abundance; VBR: viruses-to-bacteria ratio; DMS: dimethylsulfide; PON: particulate organic nitrogen; POC: particulate organic carbon; A_T: total alkalinity.

Correlation coefficient	Combined environmental factors	Correlation coefficient	Single environmental factor
0.452	Salinity, DO, BA, VBR, DMS	0.305	Salinity
0.452	Salinity, DO, BA, VBR, PON	0.305	DO
0.450	Salinity, DO, BA, VBR, POC	0.294	BA
0.450	Salinity, DO, BA, VBR	0.265	A_T
0.445	Salinity, DO, BA, VBR, A_T	0.242	DMS

concentration. Afterwards, taxonomic richness and diversity index increased again until $t20$–$t24$. The second peak and trough of apparent bacterial diversity were delayed compared to Chl *a*. During the last days, the values of these parameters increased again until the termination of the experiment (Fig. 1). Similar to the Chl *a* pattern, the minimum apparent bacterial diversity and taxonomic richness gradually increased during the whole experimental period.

The temporal development of the maximum taxonomic richness (S_{max}) and diversity index (H_{max}) are important parameters for a description of the dynamics of bacterial community diversity. In our study, S_{max} and H_{max} appeared at various dates in Phase 3 after the second Chl *a* minimum and varied from 27–35 and 2.725–3.180, respectively, in the nine mesocosms (Fig. 2). Significant differences of S_{max} (independent *t* test, $p = 0.039$) and H_{max} (independent *t* test, $p = 0.005$) were observed between the three highest pCO_2 treatments (M6, 5, 9) and other pCO_2 treatments. The S_{max} (27–29) and H_{max} values (2.725–2.906) in the three highest pCO_2 treatments were lower than in the other treatments.

The bacterial community composition (T-RFLP patterns) obtained for the nine mesocosms at each time point of sampling were generally similar (e.g., see Fig. 3 for the T-RFLP patterns of $t30$ samples). The numbers and positions of T-RFs were similar among mesocosms, although the peak heights varied. The MDS analysis of the T-RFLP patterns with double enzyme digestion (Msp I and Rsa I) showed no clear difference between samples from each individual mesocosm (Fig. 4). This was verified using T-RFLP analysis with single enzyme digestion (Msp I, Fig. S1). On the contrary, the MDS plots of T-RFLP analysis with double or single enzyme digestion revealed a temporal development of bacterial communities during the 30 day incubation (Figs. 4 and S1). The bacterial community structure gradually changed with the incubation period. Samples collected at adjacent dates grouped together on the MDS plot while the most distinctive comparisons were those from the onset and termination of the experiment (Figs. 4 and S1). This pattern, i.e., a clear temporal, but no pCO_2 effect, as observed in MDS plots was also demonstrated by the ANOSIM analysis based on the matrix of T-RF position and peak area (Tables S1 and S2). However, MDS plotting of the samples with maximum bacterial diversity showed that samples from three highest pCO_2 treatments grouped together, but were separated from the other samples (Fig. 2).

The BIOENV analysis was applied to investigate the potential effects of environmental parameters on the observed bacterial community structure (Table 1). Generally,

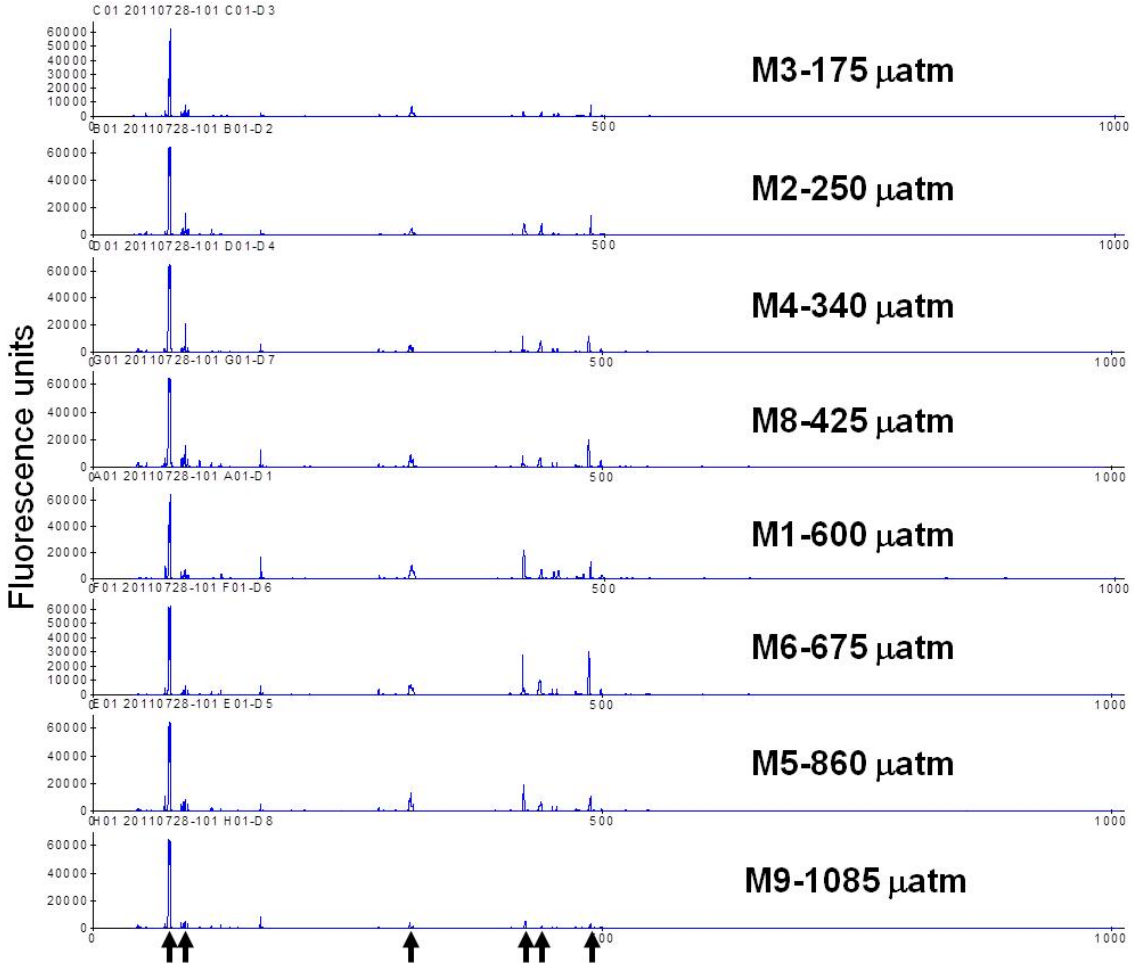

Fig. 3. Bacterial community structure after 30 day incubation revealed using T-RFLP analysis. M7 sample is absent since the mesocosm was removed before *t*30. Six T-RFs identified by in silico digestion of cloned 16S rRNA gene sequences are shown with arrows (See Fig. 5 for their phylogenetic assignment).

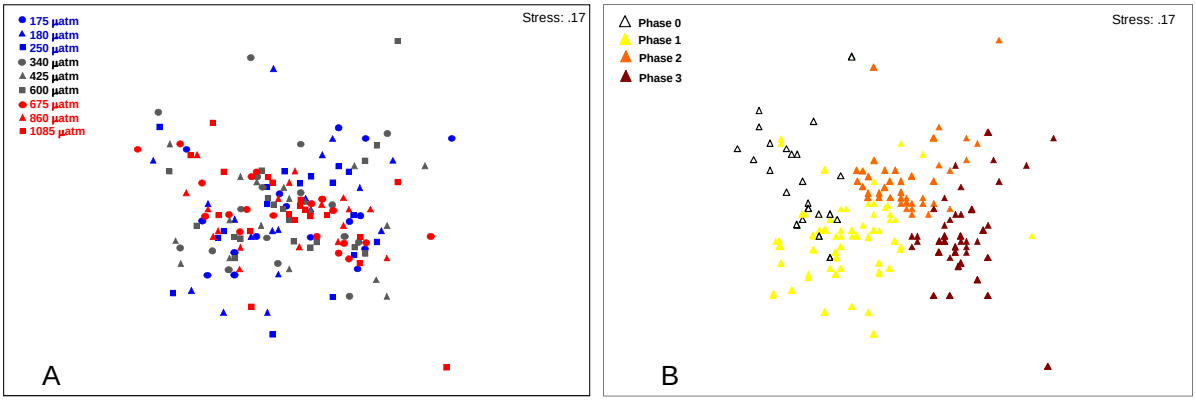

Fig. 4. MDS plots, based on double enzyme digested T-RFLP analysis, showing bacterial community dynamics during the ocean acidification mesocosm experiment. **(A)** low, intermediate and high pCO_2 treatments are displayed with blue, dark and red symbols, respectively, emphasising on the gradient pCO_2 treatments; **(B)** MDS plotting with same dataset as **(A)** emphasised on temporal development. Phases 0–3 are displayed with hollow, yellow, orange and maroon symbols, respectively. Samples collected from different experimental days within same phase are shown in same colour.

Table 2. Major OTUs (operational taxonomic units) and clone numbers observed in clone library analysis. The taxonomic assignment of each OTU was based on RDP Classifier and GenBank Blastn analysis.

OTUs	Taxonomic groups	M3-175 µatm	M2-250 µatm	M4-340 µatm	M8-425 µatm	M1-600 µatm	M6-675 µatm	M5-860 µatm	M9-1085 µatm	Total
Cryobacterium-like	*Actinobacteria*	16	30	19	18	57	6	14	13	173
Ilumatobacter	*Actinobacteria*	20	8	10	14	1	12	13	10	88
Owenweeksia	*Bacteroidetes*	2	1	3	0	0	0	1	1	8
Owenweeksia-like-1	*Bacteroidetes*	0	2	7	5	1	13	10	4	42
Owenweeksia-like-2	*Bacteroidetes*	7	0	1	0	0	0	0	1	9
Ulvibacter	*Bacteroidetes*	1	5	2	2	0	0	1	0	11
Polaribacter	*Bacteroidetes*	4	2	3	1	0	0	0	0	10
Fluviicola	*Bacteroidetes*	2	0	1	0	0	1	1	0	5
Haliscomenobacter	*Bacteroidetes*	3	0	2	2	0	2	3	0	12
Chlorophyta	*Cyanobacteria*	1	0	0	0	0	1	3	0	5
Sulfitobacter-1	*Proteobacteria* (α-)	0	2	1	4	0	0	0	4	11
Sulfitobacter-2	*Proteobacteria* (α-)	0	9	11	4	4	8	9	8	53
Loktanella	*Proteobacteria* (α-)	4	4	9	3	1	2	6	5	44
Pelagibacter	*Proteobacteria* (α-)	1	0	1	6	3	3	9	5	28
Octadecabacter	*Proteobacteria* (α-)	1	2	1	1	0	4	2	1	12
Hydrogenophaga-like	*Proteobacteria* (β-)	2	0	0	4	1	0	0	4	11
Methylophilus-1	*Proteobacteria* (β-)	6	0	2	5	0	6	1	6	26
Methylophilus-2	*Proteobacteria* (β-)	2	1	3	1	2	5	1	5	20
Haliea	*Proteobacteria* (γ-)	15	5	14	19	4	25	11	20	113
Gamma-1	*Proteobacteria* (γ-)	2	0	0	2	0	0	1	1	6
Gamma-2	*Proteobacteria* (γ-)	3	0	0	2	0	0	0	1	6
	Total	98	74	100	98	78	98	99	98	

the correlation between bacterial community structure and measured environmental factors was low. The highest correlation (0.452) was obtained with combined environmental factors including salinity, dissolved oxygen (DO) concentration, bacterial abundance (BA), viruses-to-bacteria ratio (VBR) and dimethylsulfide (DMS)/particulate organic nitrogen (PON) concentration. Other correlated parameters included particulate organic carbon (POC) and total alkalinity (A_T) (Table 1). Considering individual factors, the five parameters, which correlated best with community composition, were salinity, DO, BA, A_T and DMS.

3.2 Bacterial community composition revealed by clone library analysis

In total, 743 clones were obtained from eight clone libraries (74–100 clones each) constructed from the samples collected on $t30$ to investigated the final responses of bacterial community to 30 day artificial CO_2 manipulation (Table 2). Sequences of *Proteobacteria*, *Actinobacteria* and *Bacteroidetes* dominated all clone libraries. At the family level, the *Microbacteriaceae*, *Rhodobacteraceae* and *Alteromonadaceae* were the major groups. Based on a definition of operational taxonomic units (OTU) as 97 % similarity of the 16S rRNA gene sequence, there were 13–27 OTUs in each clone library (Fig. S2). The phylogenetic assignment and number of clones of each OTU are shown in Table 2. *Cryobacterium*, *Haliea*, *Ilumatobacter*, *Sulfitobacter* and *Loktanella* related OTUs were the five most abundant ones. We did not observe a clear trend of apparent bacterial diversity (number of OTUs) versus pCO_2 concentrations (data not shown). Although LIBSHUFF analysis showed significant difference in various pair comparisons of the clone library, there was no statistical evidence suggesting a pCO_2-related effect (Table S3). The difference among clone libraries was probably related to the fact that the relatively small sampling size (< 100 clones) in the clone library analysis was insufficient to capture the true diversity, as shown by the unsaturated asymptotic rarefaction curves in Fig. S2. Similar to the T-RFLP analysis, rarefaction analysis did not reveal clear diversity changes along the pCO_2 gradient. Although it is hard for us to predict responses of specific bacterial genotypes to ocean acidification based on clone library analysis, some OTUs seemed to be affected by pCO_2 manipulation (Table 2). For example, *Polaribacter* OTUs (*Bacteroidetes*) were only found in the four lowest pCO_2 mesocosms, but not in the four highest pCO_2 treatments. In contrast, we observed highest abundance of *Pelagibacter* OTU (*Alphaproteobacteria*) in the higher pCO_2 mesocosms.

The obtained sequences were *in silico* digested using the restriction enzymes Msp I and Rsa I for possible phylogenetic assignment to the T-RFs observed for $t30$ samples. In total, we successfully attributed six major T-RFs (see Fig. 3 for their positions), accounting for 73.8–86.6 % of the total peak area of each sample (Fig. 5), to *Alphaproteobacteria* (2 T-RFs), *Bacteroidetes* (2 T-RFs), *Actinobacteria* (1 T-RF) and *Gammaproteobacteria* (1 T-RF). A T-RF of 72–75 bp was the largest peak (44.2 ± 14.9% of total peak area, $n = 8$)

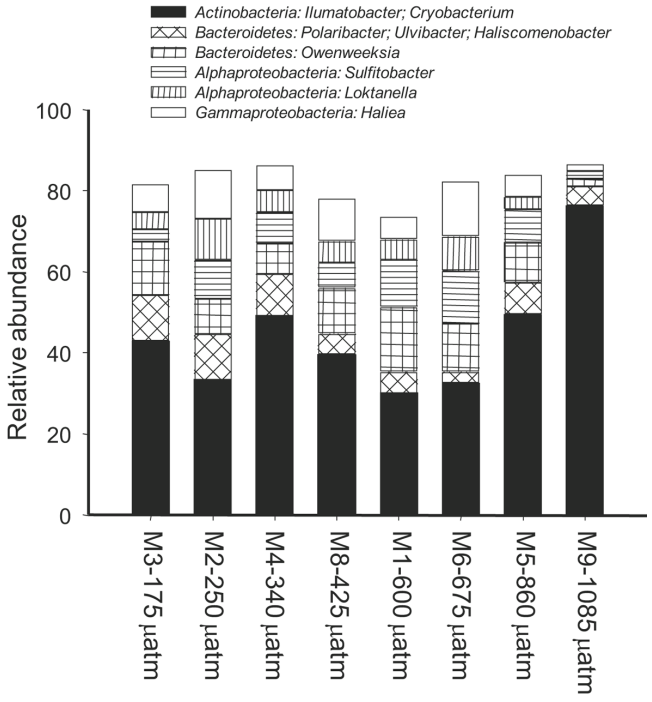

Fig. 5. Bacterial community structure after 30 day incubation with different pCO_2 treatments revealed by combined analysis of clone library and T-RFLP analysis. The phylogenetic assignment of major peaks in T-RFLP profiling was performed by in silico digestion of sequences from clone library. The relative abundance of different phylogenetic groups in each sample was calculated based on the percentage of their peak area to total peak area of the T-RFLP profile. See the Materials and Methods for details.

in all $t30$ samples, especially in M9 (Figs. 3 and 5). The e-digestion analysis of clone library sequences suggested that two *Actinobacteria* groups (*Ilumatobacter* and *Cryobacterium*) produced this T-RF. This was supported by the finding that the clone libraries were dominated by clones affiliated to these two *Actinobacteria* groups (Table 2). Several *Bacteroidetes* sequences (*Polaribacter*, *Ulvibacter*, *Haliscomenobacter* and *Owenweeksia*) produced two major T-RFs located at 86–92 bp and 308–313 bp. A negative linear correlation ($R^2 = 0.62$) between the relative abundance of *Bacteroidetes* T-RFs and pCO_2 levels was observed. The T-RFs at 420–424 bp and 436–440 bp probably originated from the alphaproteobacterial genera *Sulfitobacter* and *Loktanella*, respectively. The second most abundant OTU (*Haliea* of the *Gammaproteobacteria*) in the clone library contributed to the T-RF of 485–488 bp (Figs. 3 and 5). There was no clear trend of relative abundance of *Alphaproteobacteria* (individual or combined) and *Gammaproteobacteria* along the gradient of pCO_2 levels.

4 Discussion

4.1 Temporal development of the bacterial community

Generally, MDS analysis of T-RFLP patterns revealed significant temporal variations of BCC and the trend of apparent bacterial diversity and taxonomic richness seemed to be influenced by the variation of Chl *a* during the whole experimental incubation (Fig. 1). The temporal dynamics of bacterial community was confirmed by other two companion studies with different sampling and DNA fingerprinting strategies for both particle-attached and free-living bacterial populations (Roy et al., 2013; Sperling et al., 2013), This suggests that in our mesocosm experiment, the general heterotrophic bacterial community was tightly related with ecosystem productivity. Coupling of the bacterial community and the phytoplankton development is frequently observed in natural or experimental systems (Allgaier et al., 2008; Azam et al., 1983; Duarte et al., 2005). Heterotrophic bacterial activities, including protein production and extracellular enzyme activity, were closely coupled with phytoplankton productivity in the Svalbard mesocosm experiment (Piontek et al., 2013). In the PeECE II ocean acidification experiment, Arnosti et al. (2011) observed diverged BCC in the late-bloom phase of phytoplankton development and related this to extracellular enzyme activities associated with phytoplankton development with different pCO_2 treatments. In the present EPOCA ocean acidification experiment, bacterial activity co-varied with organic production, followed by a breakdown of picophytoplankton population, in post-bloom phase (Brussaard et al., 2013; Engel et al., 2012; Piontek et al., 2013). Therefore, the dynamics of bacterial community (including diversity and BCC) in our incubation could reflect the competition between different bacterial groups for labile dissolved organic matter released by phytoplankton. Furthermore, considering that there is no similar temporal trend of the development of heterotrophic bacterial abundance (Brussaard et al., 2013), strong top-down control of bacterioplankton biomass likely occurred in the mesocosm, which should contribute to the variation of BCC. This is supported by the fact that multiple biological parameters, including those associated with viruses (VBR) and phytoplankton (DMS), correlated to BCC dynamics in the BIOENV analysis (Table 1). This was verified by the investigation of particle-attached and free-living BCC in two accompanying studies (Roy et al., 2013; Sperling et al., 2013). Therefore, these studies showed that the cascading trophic interactions were likely a key driver of the response of heterotrophic bacterial to pCO_2 perturbation.

4.2 The effects of pCO_2 on bacterial community structure

The lack of a clear pCO_2 effect on general bacterial community composition was demonstrated by different molecular techniques (this study and Sperling et al., 2013; Roy et al.,

2013) in the EPOCA experiment and in a similar mesocosm experiment performed in Bergen (Newbold et al., 2012). Our BIOENV analysis also showed that organic and inorganic parameters contributed in a complex way to BCC dynamics (Table 1). This indicates that the increase of pCO_2 levels and its chemical consequences in the ocean might not directly affect the main structure of the marine bacterial assemblage and seem to support the null hypothesis (Joint et al., 2010) that the general bacterial community is not fundamentally different under high CO_2/low pH conditions.

In our study, however, possible pCO_2 effects on BCC were observed for the developing process of bacterioplankton during incubation (Fig. 2). High pCO_2 treatments significantly reduced S_{max} and H_{max} and changed BCC during bacterioplankton development. Our study also indicated a threshold of the pCO_2 level between 600–675 µatm which caused observed response of bacterioplankton development to ocean acidification. Such a change of bacterioplankton community behaviour can probably only be documented in long-term incubations with high sampling frequency, which was not carried out in previous studies (e.g., Allgaier et al., 2008; Newbold et al., 2012). In addition, a negative relationship between pCO_2 level and relative abundance (peak area) of *Bacteroidetes* T-RFs was observed in T-RFLP analysis. *Bacteroidetes* is an important consumer of high molecular weight (HMW) DOM in the ocean (Kirchman, 2002). They are major heterotrophic inhabitants on marine particles as well, contributing to the degradation of particulate organic matter (POM) and TEP (Zhang et al., 2007; Kirchman, 2002). The possible stimulation of POM/TEP production by phytoplankton at high pCO_2 (Liu et al., 2010) and the decline of their heterotrophic consumers (e.g., *Bacteroidetes*) might influence the biological carbon pump and subsequent carbon sequestration in the ocean sediment. Microbial communities with a reduced abundance of *Bacteroidetes* might result in a reduced HMW DOM consumption and transformation in sea water, thus, potentially affecting the efficiency of the microbial carbon pump (Jiao et al., 2010). It is noteworthy that Roy et al. (2013) did not observe a similar negative relationship between *Bacteroidetes* sequences and pCO_2 level using sequencing of barcode bacterial 16S rRNA gene PCR products. No significant response of *Bacteroidetes* to pCO_2 treatment was detected in the Bergen mesocosm experiment (Newbold et al., 2012). Therefore, further quantitative and *Bacteroidetes* specific analysis (e.g., fluorescence in situ hybridisation or real time PCR) is required.

Metagenomic analysis along a vertical profile in the oligotrophic ocean showed that representatives of the *Alphaproteobacteria* and *Gammaproteobacteria* are distributed in waters covering a wide range of natural pH conditions (DeLong et al., 2006). In our study, the relative abundance of *Alphaproteobacteria* and *Gammaproteobacteria*, revealed using T-RFLP analysis, did not vary with the level of acidification, suggesting that these two dominating marine bacterial phylogenetic groups had enough genetic or metabolic plasticity to compensate for lower pH conditions. However, considering the contrasting distribution of *Polaribacter* and *Pelagibacter* in the clone library analysis, there is the possibility that ocean acidification might change the relative contribution of some phylogenetic lineages in the *Alphaproteobacteria* and *Gammaproteobacteria*. In addition, particle-attached and free-living bacteria responded differently to pCO_2 treatments in the EPOCA experiment (Roy et al., 2013; Sperling et al., 2013), as well as in other ocean acidification investigations (Allgaier et al., 2008; Arnosti et al., 2011). These observations demonstrated divers responses of marine bacterioplankton to ocean acidification and urged further investigations on different phylogenetic and ecological groups.

5 Outlook

Our study, as well as the other two paralleled studies (Roy et al., 2013; Sperling et al., 2013), shed light on the effects of ocean acidification on bacterial community structure in the Arctic Ocean, demonstrating a general resilience of the major bacterial phylogenetic groups under various high pCO_2 conditions. However, the potential restructuring of the BCC during bacterioplankton development as a result of ocean acidification could have a direct or indirect influence on marine organic carbon cycling. Although there is evidence showing that ocean acidification potentially affects the production of DOM, TEP and POM (Liu et al., 2010), few studies have investigated the fate of organic matter in the acidified ocean (de Kluijver et al., 2010; Kim et al., 2011). As the major component incorporating organic substrates in the marine ecosystem, heterotrophic bacteria should be given more attention in the ocean acidification studies. Bacterial extracellular enzyme activity, which directly affects the degradation of organic matter, was shown to be related with pCO_2 levels (Arnosti et al., 2011; Piontek et al., 2013). The responses of specific bacterial phylogenetic or functional lineages and the development of bacterial community to different pCO_2 conditions, as revealed by the present study, might have contributed to the dynamics of extracellular enzyme activity during the incubation period (Piontek et al., 2013). Future studies linking the diversity, activity and ecological function of marine bacterioplankton have to be conducted, in order to improve our understanding of microbial mediated marine carbon cycling (e.g., the biological pump and microbial carbon pump) under high pCO_2 condition. Furthermore, considering the tight coupling of heterotrophic bacteria and phytoplankton in our mesocosm study, pCO_2 manipulation experiments performed without autotrophs are needed to elucidate the direct response of the bacterioplankton to ocean acidification.

Supplementary material related to this article is available online at: http://www.biogeosciences.net/10/3679/2013/bg-10-3679-2013-supplement.pdf.

Acknowledgements. This work is a contribution to the "European Project on Ocean Acidification" (EPOCA) which received funding from the European Community's Seventh Framework Programme (FP7/2007–2013) under grant agreement no. 211384. We gratefully acknowledge the logistical support of Greenpeace International for its assistance with the transport of the mesocosm facility from Kiel to Ny-Ålesund and back to Kiel. We also thank the captains and crews of M/V *ESPERANZA* of Greenpeace and R/V *Viking Explorer* of the University Centre in Svalbard (UNIS) for assistance during mesocosm transport and during deployment and recovery in Kongsfjorden. We thank the staff of the French-German Arctic Research Base at Ny-Ålesund, in particular Marcus Schumacher, for on-site logistical support. Financial support was provided by the 973 programme (2011CB808800, 2013CB955700). R. Z. was supported by the Fundamental Research Funds for the Central Universities (2011121012). We gratefully acknowledge the help provided by the Chinese Arctic and Antarctic Administration, SOA (IC2010006). Financial support was provided by IPEV, The French Polar Institute. John Hodgkiss is thanked for his help in polishing the English in this manuscript.

Edited by: T. F. Thingstad

References

Allgaier, M., Riebesell, U., Vogt, M., Thyrhaug, R., and Grossart, H.-P.: Coupling of heterotrophic bacteria to phytoplankton bloom development at different pCO_2 levels: a mesocosm study, Biogeosciences, 5, 1007–1022, doi:10.5194/bg-5-1007-2008, 2008.

Amann, R. I., Ludwig, W., and Schleifer, K. H.: Phylogenetic identification and *in situ* detection of individual microbial cells without cultivation, Microbiol, Mol. Biol. Rev., 59, 143–169, 1995.

Arnosti, C., Grossart, H., Mühling, M., Joint, I., and Passow, U.: Dynamics of extracellular enzyme activities in seawater under changed atmospheric pCO_2: a mesocosm investigation, Aquat. Microb. Ecol., 64, 285–298, 2011.

Azam, F., Fenchel, T., Field, J. G., Gray, J. S., Meyer-Reil, L. A., and Thingstad, F.: The ecological role of water-column microbes in the sea, Mar. Ecol. Prog. Ser., 10, 257–263, 1983.

Beman, J. M., Chow, C. E., King, A. L., Feng, Y., Fuhrman, J. A., Andersson, A., Bates, N. R., Popp, B. N., and Hutchins, D. A.: Global declines in oceanic nitrification rates as a consequence of ocean acidification, Proc. Natl. Acad. Sci. USA, 108, 208–213, 2011.

Brussaard, C. P. D., Noordeloos, A. A. M., Witte, H., Collenteur, M. C. J., Schulz, K., Ludwig, A., and Riebesell, U.: Arctic microbial community dynamics influenced by elevated CO_2 levels, Biogeosciences, 10, 719–731, doi:10.5194/bg-10-719-2013, 2013.

Caldeira, K. and Wickett, M. E.: Anthropogenic carbon and ocean pH, Nature, 425, p. 365, 2003.

Clarke, K. R. and Gorley, R. N.: PRIMER v5: user manual/tutorial, PRIMER-E Ltd, Plymouth, UK, 2001.

de Kluijver, A., Soetaert, K., Schulz, K. G., Riebesell, U., Bellerby, R. G. J., and Middelburg, J. J.: Phytoplankton-bacteria coupling under elevated CO_2 levels: a stable isotope labelling study, Biogeosciences, 7, 3783–3797, doi:10.5194/bg-7-3783-2010, 2010.

DeLong, E. F., Preston, C. M., Mincer, T., Rich, V., Hallam, S. J., Frigaard, N.-U., Martinez, A., Sullivan, M. B., Edwards, R., Brito, B. R., Chisholm, S. W., and Karl, D. M.: Community genomics among stratified microbial assemblages in the ocean's interior, Science, 311, 496–503, 2006.

Dore, J. E., Lukas, R., Sadler, D. W., Church, M. J., and Karl, D. M.: Physical and biogeochemical modulation of ocean acidification in the central North Pacific, Proc. Natl. Acad. Sci. USA, 106, 12235–12240, 2009.

Duarte, C. M., Agustí, S., Vaqué, D., Agawin, N. S. R., Felipe, J., Casamayor, E. O., and Gasol, J. M.: Experimental test of bacteria-phytoplankton coupling in the Southern Ocean, Limnol. Oceanogr., 50, 1844–1854, 2005.

Engel, A., Borchard, C., Piontek, J., Schulz, K. G., Riebesell, U., and Bellerby, R.: CO_2 increases ^{14}C primary production in an Arctic plankton community, Biogeosciences, 10, 1291–1308, doi:10.5194/bg-10-1291-2013, 2013.

Fabrega, J., Zhang, R., Renshaw, J. C., Liu, W. T., and Lead, J. R.: Impact of silver nanoparticles on natural marine biofilm bacteria, Chemosphere, 85, 961–966, 2011.

Fu, F. X., Warner, M. E., Zhang, Y., Feng, Y., and Hutchins, D. A.: Effects of increased temperature and CO_2 on photosynthesis, growth, and elemental ratios in marine *Synechococcus* and *Prochlorococcus* (Cyanobacteria), J. Phycol., 43, 485–496, 2007.

Gattuso, J. P. and Hansson, L.: European Project on Ocean Acidification (EPOCA): Objectives, products, and scientific highlights, Oceanography, 22, 190–201, 2009.

Grossart, H. P., Allgaier, M., Passow, U., and Riebesell, U.: Testing the effect of CO_2 concentration on the dynamics of marine heterotrophic bacterioplankton, Limnol. Oceanogr., 51, 1–11, 2006.

Hönisch, B., Ridgwell, A., Schmidt, D. N., Thomas, E., Gibbs, S. J., Sluijs, A., Zeebe, R., Kump, L., Martindale, R. C., and Greene, S. E.: The geological record of ocean acidification, Science, 335, 1058–1063, 2012.

Hewson, I. and Fuhrman, J. A.: Improved strategy for comparing microbial assemblage fingerprints, Microb. Ecol., 51, 147–153, 2006.

Hutchins, D. A., Fu, F. X., Zhang, Y., Warner, M., Feng, Y., Portune, K., Bernhardt, P., and Mulholland, M.: CO_2 control of Trichodesmium N_2 fixation, photosynthesis, growth rates, and elemental ratios: implications for past, present, and future ocean biogeochemistry, Limnol. Oceanogr., 52, 1293–1304, 2007.

Hutchins, D. A., Mulholland, M. R., and Fu, F.: Nutrient cycles and marine microbes in a CO_2-enriched ocean, Oceanography, 22, 128–145, 2009.

IPCC: Climate Change 2007: Synthesis Report. Summary for policy makers., November, 2007.

Jiao, N., Herndl, G. J., Hansell, D. A., Benner, R., Kattner, G., Wilhelm, S. W., Kirchman, D. L., Weinbauer, M. G., Luo, T., and Chen, F.: Microbial production of recalcitrant dissolved organic matter: long-term carbon storage in the global ocean, Nat. Rev. Microbiol., 8, 593–599, 2010.

Joint, I., Doney, S. C., and Karl, D. M.: Will ocean acidification affect marine microbes?, ISME J., 5, 1–7, 2010.

Kim, J. M., Lee, K., Shin, K., Yang, E. J., Engel, A., Karl, D. M., and Kim, H. C.: Shifts in biogenic carbon flow from particulate to dissolved forms under high carbon dioxide and warm ocean conditions, Geophys. Res. Lett., 38, L08612, doi:10.1029/2011GL047346, 2011.

Kirchman, D. L.: The ecology of *Cytophaga-Flavobacteria* in aquatic environments, FEMS Microbiol. Ecol., 39, 91–100, 2002.

Lane, D.: 16S/23S rRNA sequencing, in: Nucleic acid techniques in bacterial systematics, edited by: Stackebrandt, E. and Goodfellow, M., John Wiley & Sons, New York, 115–175, 1991.

Lau, S. C. K., Thiyagarajan, V., Cheung, S. C. K., and Qian, P. Y.: Roles of bacterial community composition in biofilms as a mediator for larval settlement of three marine invertebrates, Aquat. Microb. Ecol., 38, 41–51, 2005.

Liu, J., Weinbauer, M. G., Maier, C., Dai, M., and Gattuso, J. P.: Effect of ocean acidification on microbial diversity and on microbe-driven biogeochemistry and ecosystem functioning, Aquat. Microb. Ecol., 61, 291–305, 2010.

Martiny, J. B. H., Bohannan, B. J. M., Brown, J. H., Colwell, R. K., Fuhrman, J. A., Green, J. L., Horner-Devine, M. C., Kane, M., Krumins, J. A., and Kuske, C. R.: Microbial biogeography: putting microorganisms on the map, Nat. Rev. Microbiol., 4, 102–112, 2006.

Newbold, L. K., Oliver, A. E., Booth, T., Tiwari, B., DeSantis, T., Maguire, M., Andersen, G., van der Gast, C. J., and Whiteley, A. S.: The response of marine picoplankton to ocean acidification, Environ. Microbiol., 14, 2293–2307, 2012.

Piontek, J., Borchard, C., Sperling, M., Schulz, K. G., Riebesell, U., and Engel, A.: Response of bacterioplankton activity in an Arctic fjord system to elevated pCO_2: results from a mesocosm perturbation study, Biogeosciences, 10, 297–314, doi:10.5194/bg-10-297-2013, 2013.

Riebesell, U.: Effects of CO_2 enrichment on marine phytoplankton, J. Oceanogr., 60, 719–729, 2004.

Riebesell, U., Czerny, J., von Bröckel, K., Boxhammer, T., Büdenbender, J., Deckelnick, M., Fischer, M., Hoffmann, D., Krug, S. A., Lentz, U., Ludwig, A., Muche, R., and Schulz, K. G.: Technical Note: A mobile sea-going mesocosm system – new opportunities for ocean change research, Biogeosciences, 10, 1835–1847, doi:10.5194/bg-10-1835-2013, 2013.

Roy, A.-S., Gibbons, S. M., Schunck, H., Owens, S., Caporaso, J. G., Sperling, M., Nissimov, J. I., Romac, S., Bittner, L., Mühling, M., Riebesell, U., LaRoche, J., and Gilbert, J. A.: Ocean acidification shows negligible impacts on high-latitude bacterial community structure in coastal pelagic mesocosms, Biogeosciences, 10, 555–566, doi:10.5194/bg-10-555-2013, 2013.

Schulz, K. G., Bellerby, R. G. J., Brussaard, C. P. D., Büdenbender, J., Czerny, J., Engel, A., Fischer, M., Koch-Klavsen, S., Krug, S. A., Lischka, S., Ludwig, A., Meyerhöfer, M., Nondal, G., Silyakova, A., Stuhr, A., and Riebesell, U.: Temporal biomass dynamics of an Arctic plankton bloom in response to increasing levels of atmospheric carbon dioxide, Biogeosciences, 10, 161–180, doi:10.5194/bg-10-161-2013, 2013..

Sperling, M., Piontek, J., Gerdts, G., Wichels, A., Schunck, H., Roy, A.-S., La Roche, J., Gilbert, J., Nissimov, J. I., Bittner, L., Romac, S., Riebesell, U., and Engel, A.: Effect of elevated CO_2 on the dynamics of particle-attached and free-living bacterioplankton communities in an Arctic fjord, Biogeosciences, 10, 181–191, doi:10.5194/bg-10-181-2013, 2013.

Weinbauer, M., Mari, X., and Gattuso, J.: Effect of ocean acidification on the diversity and activity of heterotrophic marine microorganisms, in: Ocean Acidification, edited by: Gattuso, J. and Hansson, L., Oxford University Press, Oxford, 83–98, 2011.

Zhang, R., Liu, B., Lau, S. C. K., Ki, J. S., and Qian, P. Y.: Particle-attached and free-living bacterial communities in a contrasting marine environment: Victoria Harbor, Hong Kong, FEMS Microbiol. Ecol., 61, 496–508, 2007.

Zuur, A. F., Ieno, E. N., and Elphick, C. S.: A protocol for data exploration to avoid common statistical problems, Methods Ecol. Evol., 1, 3–14, 2010.